Available online at www.sciencedirect.com
ScienceDirect
Biochimica et Biophysica Acta 1773 (2007) 1583–1588
Biochimica et Biophysica Acta BBA
www.elsevier.com/locate/bbamcr

Cellular binding, motion, and internalization of synthetic gene delivery polymers

Gaelen T. Hess [a], William H. Humphries IV [b], Nicole C. Fay [b], Christine K. Payne [b,*]

[a] *Biophysics Program, Harvard University, Cambridge, MA 02138, USA*
[b] *School of Chemistry and Biochemistry and Petit Institute for Bioengineering and Bioscience, Georgia Institute of Technology, Atlanta, GA 30332, USA*

Received 26 February 2007; received in revised form 9 July 2007; accepted 16 July 2007
Available online 7 August 2007

Abstract

Using fluorescence microscopy we have tracked the cellular binding, surface motion, and internalization of polyarginine and polyethylenimine, cationic ligands used for gene and protein delivery. Each ligand was complexed with a quantum dot to provide a photostable probe. Transfection with exogenous DNA was used to relate the observed motion to gene delivery. Cell surface motion was independent of sulfated proteoglycans, but dependent on cholesterol. Cellular internalization required sulfated proteoglycans and cholesterol. These observations suggest that sulfated proteoglycans act as cellular receptors for the cationic ligands, rather than only passive binding sites. Understanding the interaction of polyarginine and polyethylenimine with the plasma membrane may assist in designing more efficient gene delivery systems.

Keywords: Heparan sulfate proteoglycan; Cholesterol; Gene delivery; Fluorescence microscopy; Single particle tracking; Quantum dot

1. Introduction

Cationic polymers and peptides are becoming increasingly important as vectors to deliver genes, proteins, and other molecular cargo to cells. Two promising vectors are polyarginine (PA) and polyethylenimine (PEI) [1,2]. These vectors can be conjugated to proteins and other large molecules or electrostatically complexed with anionic DNA [3–8]. The net charge of both the PA and PEI complexes is positive, allowing the complex to bind to negatively charged molecules on the cell surface. Following binding, these cationic complexes undergo diffusive motion on the cell surface before internalization via endocytosis [9–13].

The motion of PA and PEI on the cell surface and within the cell can be observed directly using fluorescence microscopy and a suitable fluorescent probe. Quantum dots provide bright, photostable probes that can be combined with PA or PEI to form a highly fluorescent complex. The use of quantum dots as probes allows for long-time, continuous tracking of individual complexes. In this study, cells were treated with drugs to disrupt cell surface proteoglycans, the binding site for these ligands [12,14–16], and cholesterol, essential for the dynamics of the plasma membrane. Cationic ligand-quantum dot complexes were tracked under these conditions to determine the effect on motion and internalization. To this end, fluorescence microscopy provides an ideal method to isolate and observe individual steps of the internalization process. Transfection with exogenous DNA was used to relate the observed motion to the overall process of gene delivery. Although the quantum dot complexes are smaller than the PEI–DNA complexes used for gene delivery, recent work has shown that both complexes utilize the same endocytic pathway [16].

2. Materials and methods

2.1. Cell culture

BS-C-1 cells (ATCC) were maintained in a 5% carbon dioxide environment in Dulbecco's modified Eagle's medium (Invitrogen) with 10% (v/v) fetal bovine serum at 37 °C. Cells were passaged every 3 days. For fluorescence imaging, cells were cultured to 80% confluency in 60 mm glass-bottomed Petri dishes (MatTek). Imaging experiments were carried out in phenol red-free minimum essential medium (Invitrogen).

* Corresponding author. Tel.: +1 404 385 3125; fax: +1 404 385 6057.
E-mail address: christine.payne@chemistry.gatech.edu (C.K. Payne).

0167-4889/$ - see front matter © 2007 Elsevier B.V. All rights reserved.
doi:10.1016/j.bbamcr.2007.07.009

2.2. Quantum dot conjugation

Quantum dots (QDs, Invitrogen) with 705 nm emission were conjugated to either biotin-tagged polyarginine (PA–QDs, $R=8$, as determined by mass spectrometry), according to the manufacturer's instructions (QTracker Protocol), or polyethylenimine (22 kDa, linear, jetPEI, Bridge Bioscience Corporation) at a ratio of 3.75×10^4 nitrogen PEI residues to QDs. PEI was electrostatically bound to streptavidin-conjugated quantum dots (PEI–QDs), an interaction that remained intact throughout the duration of the experiment, described below. In comparison to standard fluorescent dyes for DNA, the QDs provide a brighter, longer-lived fluorescent probe. As described below, QDs that were not complexed with PA or PEI were not internalized by the cell. For imaging, both PA– and PEI–QDs were added to the cell culture at a concentration of 100 pM.

The hydrodynamic radii of the QD complexes was measured with dynamic light scattering (DLS, Protein Solutions) using a cummulant analysis method (Protein Solutions). Measurements were carried out at 20 °C and 37 °C and averaged over a minimum of 20 points with 10 s integration times. Streptavidin-QDs, the basic QD structure for each of the complexes, measured 14.1±3.8 nm at 20 °C and 16.1±6.5 nm at 37 °C. This is in good agreement with the 15.7±3.7 nm hydrodynamic radius measured by N.C. Cady et al. at 25 °C [17]. PEI–QDs measured 27.4±9.4 nm at 20 °C and 28.7±9.7 nm at 37 °C. Time-dependent measurements showed that the radius of the PEI–QDs, measured at 20 °C, increased from 27.4±9.4 immediately following the 30-min room temperature incubation required for preparation to 29.0±13.3 nm following another 60 min incubation at room temperature. This indicates that the PEI–QD complexes remained intact and did not aggregate over a 1 h period. We were unable to use DLS to measure the radius of the PA–QD complexes. Invitrogen specifies a radius of 11 nm, measured by size exclusion chromatography. Despite much discussion with Invitrogen, we have been unable to resolve the reason for the difficulty of DLS measurements. Based on our measurement of streptavidin–QDs and PEI–QDs, we expect the hydrodynamic radius of the PA–QDs to be approximately 20 nm.

2.3. PEI–DNA conjugation and gene delivery

In addition to QDs, PEI was also complexed with DNA to measure the efficiency of gene delivery. In this case, PEI was complexed with β-galactosidase DNA (Promega) with a ratio of 8 PEI nitrogen residues to 1 DNA phosphate residue (N:P=8) in 200 μL of 150 μM NaCl as specified by the jetPEI protocol. The hydrodynamic radii of the PEI–DNA complexes was 311.2±164.1 nm, measured at 37 °C. Hydrodynamic radii of PEI–DNA complexes are very sensitive to salt concentrations during preparation and previous measurements range from 50 nm [18] to 236 nm [19]. Despite the larger size of the PEI–DNA complexes, previous work has shown that the same endocytic pathway is used by PEI–siRNA and DNA complexes and PA–QD complexes [16].

For measurements of transfection efficiency, a total of 3 μg DNA, complexed with PEI, was added to each well of a 6-well plate. Cells were incubated with the PEI–DNA for 2 h at which time 50 μg/mL dextran sulfate (9000–20,000 Da, Sigma-Aldrich) was added to each well to dissociate the PEI from the DNA thereby stopping transfection. This allowed 2 h for internalization of the PEI–DNA complex. Any complexes remaining on the cell surface were dissociated and inactivated. The dissociation with dextran sulfate has also been observed using two-color fluorescence imaging and ethidium bromide staining (data not shown). Transfection efficiency was recorded at 24 h by measuring the expression of β-galactosidase via the conversion of o-nitrophenyl-β-D-galactoside to o-nitrophenol (Promega, β-galactosidase assay) and normalized against the concentration of cell lysate. As a control, cells in which PEI–DNA was added simultaneously with dextran sulfate showed 0% transfection efficiency.

Unfortunately, PEI–DNA, with DNA labeled with intercalating dyes such as TOTO-3 (Invitrogen), and PEI-siRNA, with the siRNA labeled with Cy5 (Dharmacon), were not sufficiently bright and photostable for the continuous, long time tracking necessary to characterize motion on the cell surface.

2.4. Drug treatments

The incubation of cells with sodium chlorate, 80 mM for 24 h prior to experiments, was used to inhibit ATP-sulfurylase thereby preventing the sulfation of proteoglycans [20]. This method has been used previously in the study of gene delivery vectors and appears to be specific in the targeting of proteoglycans [14,21]. The efficiency of this treatment was tested with an antibody against heparan sulfate proteoglycans [16]. No changes in cell morphology were observed following sodium chlorate treatment and, as a control to test the viability of non-proteoglycan binding sites, binding of transferrin was unaffected [16]. After the 24 h pretreatment, sodium chlorate was removed from the medium immediately prior to the addition of PA–QDs or PEI–DNA. Methyl-β-cyclodextrin (MβCD) was used to sequester cholesterol from the plasma membrane [22]. Cells were pretreated with 2 mM MβCD for 30 min prior to experiments. All drugs were purchased from Sigma-Aldrich.

2.5. Measurement of internalization

Internalization of PA–QDs was measured using software written to count the number of QDs present in cells following the dextran sulfate treatment described below. The numbers reported for internalization measurements reflect the number of QDs averaged over 10–20 cells. For each drug treatment, individual cells showed approximately the same extent of internalization meaning that the drug treatments affected all cells equally. Large aggregates, >1 μm, of PA–QDs were occasionally observed on the cell surface and these were not included in the analysis. The identification of a single QD is typically determined by the observation of blinking as it is unlikely that multiple quantum dots will each enter a dark state simultaneously. While blinking is observed for PA–QDs on the cell surface, internalized PA–QDs show reduced blinking, likely due to the formation of small aggregates of PA–QDs within individual endosomes [23]. It is unclear if the formation of small aggregates occurs immediately prior to internalization, possibly through a clustering mechanism, or due to rapid fusion of the initial endosomes.

2.6. Removal of cationic ligands-quantum dots from the cell surface

Imaging did not exceed 10 min following addition of PA–QDs to the cell culture. At this time the majority of quantum dots were not yet internalized by the cell and remained on the cell surface. The extent of internalization was measured using a high concentration, 100 μg/mL, of anionic dextran sulfate to remove quantum dots from the cell surface. The addition of this high concentration of dextran sulfate dissociated quantum dots from the membrane allowing them to be rinsed from the cell culture, as tested by cold-binding experiments at 4 °C. Any PA–QDs that were internalized remained visible after rinsing. Using this method, we measured that 13% of the PA–QDs were internalized within the period images were collected. Internalized PA–QDs displayed rapid, directed motion indicative of microtubule-dependent transport and were not included in the cell surface motion analysis [24,25].

2.7. Fluorescence imaging

PA– and PEI–QDs were excited with a 532 nm diode laser (Crystalaser). A polychroic beamsplitter (Chroma) designed to reflect at 520–550 nm was used to direct the laser line onto the cells. The fluorescent emission at 705 nm was collected by an oil-immersion objective (N.A.=1.45, 60X, Olympus) using an IX70 Olympus microscope in an epifluorescent configuration and imaged onto a CCD camera (Roper Scientific, CoolSnap HQ). Leak through of the 532 nm laser line was removed with a 665 nm longpass filter (Chroma). Images were recorded at a rate of 2 Hz for a period of 10 min. Experiments were conducted at 37 °C and 20 °C. Temperature was controlled by a water bath-heated stage plate and objective collar.

2.8. Data analysis

A time series of fluorescence images was used to determine the speed of the PA– or PEI–QDs on the cell surface. PA–QDs are used as an example to explain the method. Data analysis began with the random selection of 7–10 PA–QD complexes on the surface of each cell. These randomly chosen PA–QD complexes were tracked over a period of 10 min and the distance traveled within each 500 ms period was recorded and converted to speed. The speed of the PA–QD at each step was used to construct a probability distribution in which the x-axis shows the speed of each step and the *y*-axis shows the percent of PA–QDs with a specific speed within the 500-ms time step. It is important to note that this

is not a histogram for a single PA–QD, but instead a probability distribution of for a collection of PA–QDs randomly distributed on the cell surface. Rather than selecting a single PA–QD as an example, we examined multiple, randomly chosen, PA–QDs as a population. While we estimate that 2000 steps are sufficient for a representative distribution, larger data sets were collected for PA–QDs on untreated cells, as these data were used as a point of comparison for all other experiments. The distribution was truncated at 1.5 μm/s for visualization. All values were included in the analysis.

3. Results and discussion

3.1. Motion of polyarginine and polyethylenimine-quantum dots on the cell surface

Polyarginine–quantum dots (PA–QDs) added to cells at 37 °C showed a distribution with a mean of .41 μm/s and a mode of 0.08 μm/s (Fig. 1A). The distribution constructed for PA–QDs at 37 °C consists of speeds recorded from 24 cells with a total of 23,247 steps. As described above, this motion occurred on the cell surface and did not show any directionality indicative of microtubule-dependent motion. The distribution observed for PA–QDs at 37 °C serves as a comparison for subsequent measurements. The observed motion was temperature-dependent. At 20 °C, a temperature at which the mobility of the plasma membrane is reduced, motion continued on the cells surface, but the distribution of speeds narrowed and shifted to slower speeds with a mean of 0.30 μm/s and a mode of 0.04 μm/s (Fig. 1B). Conjugation of quantum dots with PEI (PEI–QDs), instead of PA, resulted in a similar distribution to that of PA–QDs (Fig. 1A and C, both 37 °C). In the absence of PA or PEI, QDs bound to the plasma membrane and showed limited motion (Fig. 1D, 37 °C), similar to that of cells at 20 °C. Without conjugation to a cationic ligand the QDs were not internalized by the cell.

3.2. Disrupting proteoglycans does not inhibit motion on the cell surface

Proteoglycans, specifically heparan sulfate proteoglycans, have been shown to be necessary for cellular internalization of

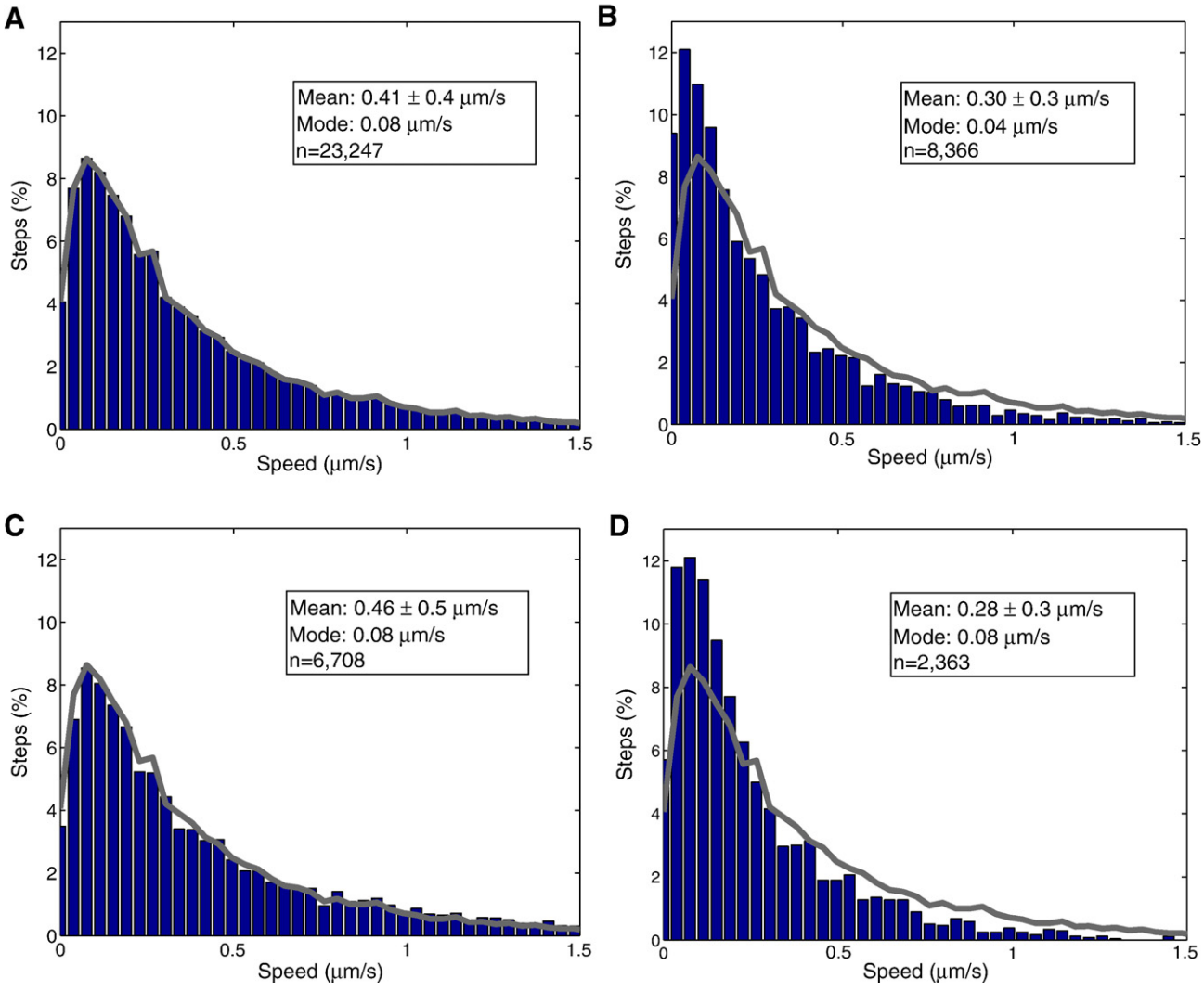

Fig. 1. Motion of cationic ligands on the cell surface. (A) Distribution of speeds for PA–QDs at 37 °C. The gray line is a direct plot of the data points and is used for comparison in the following figures. (B) At 20 °C the distribution of PA–QD speeds is shifted to slower speeds as compared to 37 °C (gray line). (C) PEI–QDs at 37 °C show a similar distribution to that of PA–QDs (gray line). (D) In the absence of PA or PEI, QDs show limited motion and are not internalized by the cell, 37 °C.

cationic vectors including; polylysine, spermine, polyarginine, and polyethylenimine [12,14–16,26]. The sulfate groups of the proteoglycans provide a dense region of negative charge on the cell surface, an ideal binding site for cationic ligands [27]. To test the role of proteoglycans in cell surface motion, PA–QDs were tracked on the cell surface in the absence of negatively charged sulfate groups following sodium chlorate treatment. Sodium chlorate inhibits the activity of ATP–sulfurylase, an enzyme that leads to the sulfation of proteoglycans in cells [20]. PA–QDs were added to cells immediately before imaging. Importantly, the medium was not replaced after the PA–QDs were added to the cells, i.e. the cells were not washed.

Following addition to the sodium chlorate treated-cells, PA–QDs bound to and moved on the cell surface (Fig. 2A). Surprisingly, motion on the cell surface showed strong similarities to that of untreated cells. While it had been expected that the removal of the main binding site would prevent binding or radically alter motion, the distribution showed a similar mean, 0.44 μm/s, an increased mode, 0.11 μm/s, and a broader distribution with no observed decrease in the number of PA–QDs bound to the cells. Qualitatively, this distribution reflects a slight increase in the motion of PA–QDs on the cell surface. Within the 10 min observation no differences were observed in the lengths of the trajectories for control and sodium chlorate-treated cells.

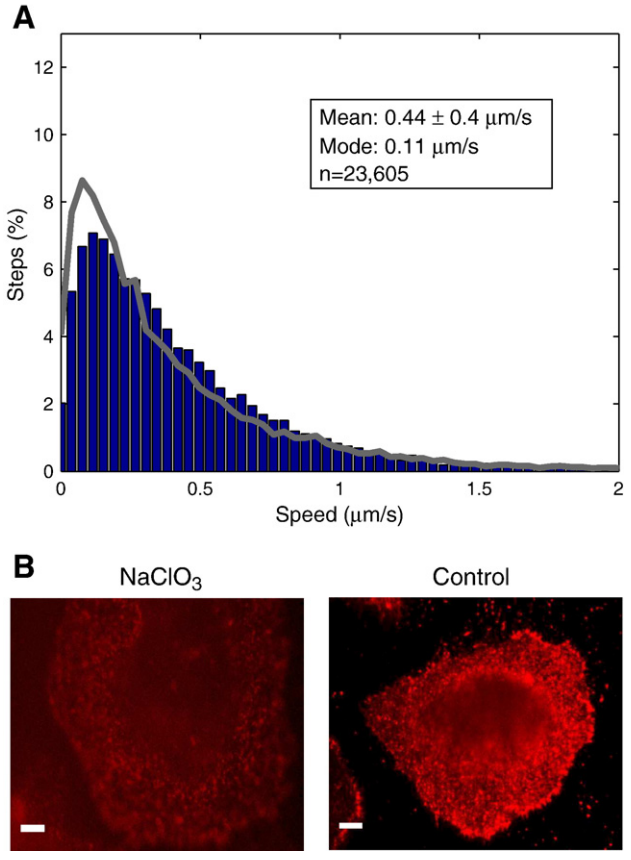

Fig. 2. The disruption of proteoglycans does not inhibit motion, but does affect binding. (A) Distribution of PA–QD speeds following sodium chlorate treatment for the removal of sulfated proteoglycans, 37 °C. The gray line shows the distribution for untreated cells. (B) PA–QD binding after washing of sodium chlorate-treated ($NaClO_3$) and control cells. Scale bars: 10 μm. The same effect is seen for PEI–QDs.

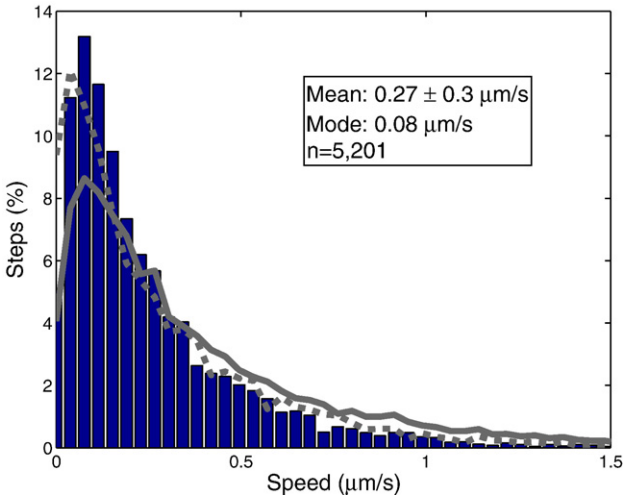

Fig. 3. Plasma membrane cholesterol is necessary for motion. The use of MβCD to sequester cholesterol resulted in a PA–QD distribution similar to that observed at 20 °C (dashed gray line) in comparison to 37 °C (solid gray line).

3.3. Disrupting proteoglycans prevents stable binding and internalization

While the motion of the PA–QDs on the cell surface was slightly increased by the removal of the proteoglycan sulfate groups, the permanent binding and internalization of PA–QDs was ultimately blocked by the sodium chlorate treatment. For control cells, PA–QDs and PEI–QDs were stably bound to the cell surface meaning the ligands remained bound to the cells following replacement of the cell culture medium (Fig. 2B, Control). In comparison, sodium chlorate treatment resulted in the dissociation of PA–QDs and PEI–QDs from the cell surface following replacement of the cell culture medium (Fig. 2B, $NaClO_3$). These results suggest a weak interaction between PA or PEI and a secondary binding site on the cell surface. There are a number of candidates for the weaker binding site responsible for binding in the absence of sulfate groups as a range of anionic ligands are present on the cell surface that may bind to PA or PEI. The observation that the distribution of motion is not strongly affected by the sodium chlorate treatment suggests that the weaker binding site may be another species of proteoglycan with similar cell surface dynamics, possibly remaining sulfated due to the selectivity of the sodium chlorate treatment [28].

Despite weak binding to the cell surface, internalization of the PA–QDs and PEI does require sulfated proteoglycans on the cell surface. This was tested in two ways. First, direct imaging was used in combination with a dextran sulfate wash. The dextran sulfate wash removed PA–QDs from the cell surface while PA–QDs that have been internalized were unaffected. One hour after the addition of PA–QDs to the cell medium, cells were washed with dextran sulfate and imaged. The internalization for untreated cells was normalized to 100%. In comparison, the majority of PA–QDs were removed from sodium

chlorate treated cells with a 64% decrease in internalization compared to the control cells. Second, the entire gene delivery process was tested by complexing PEI with β-galactosidase DNA and measuring the expression of β-galactosidase 24 h after addition to cell culture. The transfection efficiency for untreated cells is normalized to 100%. In comparison, sodium chlorate treated cells showed a 53% transfection efficiency. The internalization of a fluid phase marker, 10,000 Da TMR-labeled dextran (Invitrogen), was not inhibited by the sodium chlorate treatment.

3.4. Sequestering cholesterol inhibits motion on the cell surface

Methyl-β-cyclodextrin (MβCD) sequesters cholesterol from the plasma membrane reducing the mobility of the plasma membrane [22]. Following a 30 min pretreatment with 2 mM MβCD, cells were imaged at 37 °C using the methods described above. MβCD treatment resulted in a very different distribution of speeds in comparison to untreated cells (Fig. 3). The mean shifted downward to 0.27 μm/s and the distribution narrowed. The distribution for MβCD treated cells at 37 °C was similar to that for untreated cells at 20 °C (dashed curve).

3.5. Sequestering cholesterol prevents internalization

As with sodium chlorate, the internalization of PA–QDs in the presence of MβCD was measured by direct imaging and PEI-mediated gene delivery was determined by measuring transfection efficiency for PEI complexed with β-galactosidase DNA. Direct visualization of PA–QDs showed a 45% decrease for internalization and 35% decrease of β-galactosidase expression. This decrease in internalization was expected considering the wide range of inhibitory effects observed for MβCD treatment. Sequestering cholesterol with MβCD has been shown to have an inhibitory effect on multiple internalization pathways including; clathrin-, caveolin-, and lipid raft-mediated pathways, as well as the mobility of non-raft proteins [29–32]. Additionally, it is possible that "clustering" of the proteoglycans is necessary for the internalization of PA and PEI [33]. In this case, the inhibited mobility of the membrane would prevent clustering and block the internalization of these ligands. In short, MβCD treatment will block many internalization pathways and is used as a control to demonstrate the reduced motion and internalization associated with cholesterol sequestration.

In summary, we have used fluorescence microscopy to track the binding, cell surface motion, and internalization of the cationic ligands PA and PEI using quantum dots as fluorescent probes. The disruption of the sulfate groups of the proteoglycans revealed a surprising interaction of PA and PEI with the cell surface. The removal of the sulfate groups did not prevent a weak binding of the PA or PEI to the cell surface and did not inhibit the motion of the PA–QDs on the cell surface. Despite the weak interaction with the cell surface and a similar distribution of speeds, the internalization of PA–QDs and PEI–DNA was blocked in the absence of the sulfate groups. As expected, the removal of cholesterol inhibits both motion and internalization. The results obtained with the direct tracking of individual PA– and PEI–QDs, supported by transfection studies, are most significant in understanding the importance of sulfated proteoglycans for internalization, in addition to binding, of cationic gene delivery vectors. Unlike ligands such as transferrin or epidermal growth factor, synthetic ligands used for gene delivery do not have conjugate cellular receptors. The observation that PA and PEI complexes bind to the cell surface and exhibit similar dynamics in the absence of sulfated proteoglycans, but cannot be internalized, suggests that sulfated proteoglycans may act as true receptors for PA and PEI [16,33]. Overall, understanding the interaction of PA and PEI with the cell surface, especially in terms of receptor interactions, may assist in designing more efficient gene delivery systems and also provides a general model for the interaction of synthetic ligands with the cell surface.

Acknowledgements

This research began in the Department of Chemistry and Chemical Biology, Harvard University. The authors would like to thank Professor Xiaowei Zhuang, Harvard University, for her support of this research and Professor Andrew Lyon and Mr. Zhiyong Meng, GATech, for their assistance with dynamic light scattering experiments. N.C.F. is supported by a Merck Undergraduate Research Initiation Award and a Presidential Undergraduate Research Award from GATech. N.C.F. was also a participant in the Summer 2007 Research Experience for Undergraduates in Chemistry and Biochemistry at GATech. C.K.P. was partially supported by a Ruth L. Kirschstein National Research Service Award from the National Institutes of Health.

References

[1] P.A. Wender, D.J. Mitchell, K. Pattabiraman, E.T. Pelkey, L. Steinman, J.B. Rothbard, The design, synthesis, and evaluation of molecules that enable or enhance cellular uptake: peptoid molecular transporters, Proc. Natl. Acad. Sci. U. S. A. 97 (2000) 13003–13008.
[2] O. Boussif, F. Lezoualch, M.A. Zanta, M.D. Mergny, D. Scherman, B. Demeneix, J.P. Behr, A versatile vector for gene and oligonucleotide transfer into cells in culture and in-vivo-polyethylenimine, Proc. Natl. Acad. Sci. U. S. A. 92 (1995) 7297–7301.
[3] W.T. Godbey, K.K. Wu, A.G. Mikos, Poly(ethylenimine) and its role in gene delivery, J. Control. Release 60 (1999) 149–160.
[4] S.R. Schwarze, S.F. Dowdy, In vivo protein transduction: intracellular delivery of biologically active proteins, compounds and DNA, Trends Pharmacol. Sci. 21 (2000) 45–48.
[5] S.C. De Smedt, J. Demeester, W.E. Hennink, Cationic polymer based gene delivery systems, Pharm. Res. 17 (2000) 113–126.
[6] D.J. Mitchell, D.T. Kim, L. Steinman, C.G. Fathman, J.B. Rothbard, Polyarginine enters cells more efficiently than other polycationic homopolymers, J. Pept. Res. 56 (2000) 318–325.
[7] D.W. Pack, A.S. Hoffman, S. Pun, P.S. Stayton, Design and development of polymers for gene delivery, Nat. Rev. Drug. Discov. 4 (2005) 581–593.
[8] J.W. Fabre, L. Collins, Synthetic peptides as non-viral DNA vectors, Curr. Gene Ther. 6 (2006) 459–480.
[9] M. Debrabander, R. Nuydens, A. Ishihara, B. Holifield, K. Jacobson, H. Geerts, Lateral diffusion and retrograde movements of individual cell-surface components on single motile cells observed with nanovid microscopy, J. Cell Biol. 112 (1991) 111–124.
[10] A. Remy-Kristensen, J.P. Clamme, C. Vuilleumier, J.G. Kuhry, Y. Mely, Role of endocytosis in the transfection of L929 fibroblasts by polyethylenimine/DNA complexes, Biochim. Biophys. Acta, Biomembr. 1514 (2001) 21–32.

[11] T. Bieber, W. Meissner, S. Kostin, A. Niemann, H.P. Elsasser, Intracellular route and transcriptional competence of polyethylenimine–DNA complexes, J. Control. Release 82 (2002) 441–454.
[12] S.M. Fuchs, R.T. Raines, Pathway for polyarginine entry into mammalian cell, Biochemistry 43 (2004) 2438–2444.
[13] R. Bausinger, K. von Gersdorff, K. Braeckmans, M. Ogris, E. Wagner, C. Brauchle, A. Zumbusch, The transport of nanosized gene carriers unraveled by live-cell imaging, Angew. Chem. Int. Ed. 45 (2006) 1568–1572.
[14] K.A. Mislick, J.D. Baldeschwieler, Evidence for the role of proteoglycans in cation-mediated gene transfer, Proc. Natl. Acad. Sci. U. S. A. 93 (1996) 12349–12354.
[15] M. Belting, S. Persson, L.A. Fransson, Proteoglycan involvement in polyamine uptake, Biochem. J. 338 (1999) 317–323.
[16] C.K. Payne, S.A. Jones, C. Chen, X.W. Zhuang, Internalization and trafficking of cell surface proteoglycans and proteoglycan-binding ligands, Traffic 8 (2007) 389–401.
[17] N.C. Cady, A.D. Strickland, C.A. Batt, Optimized linkage and quenching strategies for quantum dot molecular beacons, Mol. Cell. Probes 21 (2007) 116–124.
[18] S. Choosakoonkriang, B.A. Lobo, G.S. Koe, J.G. Koe, C.R. Middaugh, Biophysical characterization of PEI/DNA complexes, J. Pharm. Sci. 92 (2003) 1710–1722.
[19] M. Thomas, Q. Ge, J.J. Lu, J.Z. Chen, A.M. Klibanov, Cross-linked small polyethylenimines: while still nontoxic, deliver DNA efficiently to mammalian cells in vitro and in vivo, Pharm. Res. 22 (2005) 373–380.
[20] P.A. Baeuerle, W.B. Huttner, Chlorate—A potent inhibitor of protein sulfation in intact-cells, Biochem. Biophys. Res. Commun. 141 (1986) 870–877.
[21] P.A. Baeuerle, W.B. Huttner, Chlorate—A potent inhibitor of protein sulfation in intact cells, Biochem. Biophys. Res. Commun. 141 (1986) 870–877.
[22] J. Pitha, T. Irie, P.B. Sklar, J.S. Nye, Drug solubilizers to aid pharmacologists—Amorphous cyclodextrin derivatives, Life Sci. 43 (1988) 493–502.
[23] X.L. Nan, P.A. Sims, P. Chen, X.S. Xie, Observation of individual microtubule motor steps in living cells with endocytosed quantum dots, J. Phys. Chem., B 109 (2005) 24220–24224.
[24] G. Apodaca, Endocytic traffic in polarized epithelial cells: role of the actin and microtubule cytoskeleton, Traffic 2 (2001) 149–159.
[25] S. Ma, R.L. Chisholm, Cytoplasmic dynein-associated structures move bidirectionally in vivo, J. Cell Sci. 115 (2002) 1453–1460.
[26] M. Belting, Heparan sulfate proteoglycan as a plasma membrane carrier, Trends Biochem. Sci. 28 (2003) 145–151.
[27] D.L. Rabenstein, Heparin and heparan sulfate: structure and function, Nat. Prod. Rep. 19 (2002) 312–331.
[28] F. Safaiyan, S.O. Kolset, K. Prydz, E. Gottfridsson, U. Lindahl, M. Salmivirta, Selective effects of sodium chlorate treatment on the sulfation of heparan sulfate, J. Biol. Chem. 274 (1999) 36267–36273.
[29] M. Edidin, The state of lipid rafts: from model membranes to cells, Annu. Rev. Biophys. Biomolec. Struct. 32 (2003) 257–283.
[30] S.K. Rodal, G. Skretting, O. Garred, F. Vilhardt, B. van Deurs, K. Sandvig, Extraction of cholesterol with methyl-beta-cyclodextrin perturbs formation of clathrin-coated endocytic vesicles, Mol. Biol. Cell 10 (1999) 961–974.
[31] A. Subtil, I. Gaidarov, K. Kobylarz, M.A. Lampson, J.H. Keen, T.E. McGraw, Acute cholesterol depletion inhibits clathrin-coated pit budding, Proc. Natl. Acad. Sci. U. S. A. 96 (1999) 6775–6780.
[32] D.E. Shvartsman, O. Gutman, A. Tietz, Y.I. Henis, Cyclodextrins but not compactin inhibit the lateral diffusion of membrane proteins independent of cholesterol, Traffic 7 (2006) 917–926.
[33] I. Kopatz, J.S. Remy, J.P. Behr, A model for non-viral gene delivery: through syndecan adhesion molecules and powered by actin, J. Gene Med. 6 (2004) 769–776.